Journal of Medicinal Chemistry Article

J. Med. Chem. **2009,** *52,* 4903–4910 **4903**
DOI: 10.1021/jm900515g

Synergistic Effect of Zanamivir−Porphyrin Conjugates on Inhibition of Neuraminidase and Inactivation of Influenza Virus

Wen-Hsien Wen,[†,∥] Mengi Lin,[‡,∥] Ching-Yao Su,[‡,§] Shi-Yun Wang,[‡] Yih-Shyun E. Cheng,*[,‡] Jim-Min Fang,*[,†,‡] and Chi-Huey Wong[‡,§]

[†]*Department of Chemistry, National Taiwan University, Taipei, 106, Taiwan,* [‡]*The Genomics Research Center, Academia Sinica, Taipei, 115, Taiwan, and* [§]*Institute of Biochemical Sciences, National Taiwan University, Taipei, 106, Taiwan.* [∥]*These authors contributed equally.*

Received April 23, 2009

New anti-influenza agents of tetravalent zanamivir on a porphyrin scaffold were synthesized. These compounds are 10 to 100 times more potent in inhibiting influenza replications even though they are somewhat less potent in neuraminidase inhibition than the monomeric zanamivir. The enhanced anti-influenza activity is probably attributable to the additional viral inactivation by singlet oxygen due to sensitization of the porphyrin moiety, which is brought in close proximity of virus by the conjugated zanamivir in a manner resembling the "magic bullet" mechanism.

Introduction

Influenza remains a major health problem. The worldwide occurrences of the fatal H5N1 avian flu and the recent outbreak of the new type H1N1 human flu have increased public awareness of the potential for global influenza pandemics. Oseltamivir phosphate[1−4] and zanamivir (**1**)[5−8] are popular drugs for the treatment of influenza. Both drugs inhibit influenza virus neuraminidase (NA[a]),[9−11] which is essential for virus propagation by cleaving the linkage between the progeny virus from the surface sialo-receptor of host cells. However, the emergence of drug-resistant influenza viruses has also caused another problem in medical treatment. In comparison, oseltamivir phosphate is more susceptible to the newly evolved resistant viruses than zanamivir.[12−21] However, zanamivir is made in powder for administration by nasospray in low bioavailability, thus modification of zanamivir to improve its therapeutic use has been pursued.[22,23] According to the structural analysis,[24,25] derivatization of zanamivir at the C-7 hydroxyl group will not substantially reduce its affinity to the active site of NA. Some zanamivir analogues by transformation of 7-OH to carbamate[22] or alkoxy groups[23] indeed possess similar or better NA inhibition. Multivalent zanamivir conjugates,[26−30] e.g., the divalent compounds **2** and **3**, have also been investigated. Although their binding strength with NA is lowered 10−20 fold, the divalent zanamivir compounds do show about 100-fold potency against influenza virus.[26−28] Moreover, the divalent zanamivir compounds can stay in lung and respiratory tracts longer than zanamivir. A long-acting neuraminidase inhibitor (LANI) is currently under phase III clinical trial.[29]

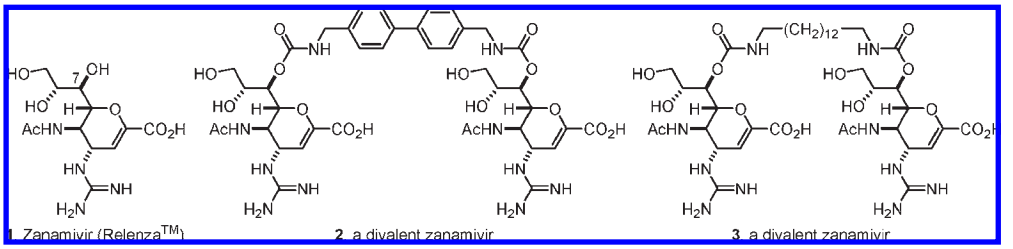

In this study, we report the new anti-influenza virus agents **4**−**6** that bear tetravalent zanamivir moieties on a porphyrin scaffold. These compounds not only showed potent NA inhibitory activity but also inactivated influenza viruses on irradiation under room light. Porphyrins and the related compounds,[31−33] e.g., Photofrin and Foscan, have been utilized as the photosensitizers to activate molecular oxygen ($^3O_2$). The activated singlet oxygen ($^1O_2$) can be applied as a highly reactive oxidant in photodynamic therapy (PDT)[31−33] to kill the cells in close proximity. PDT has been successfully used in cancer therapy and occasionally in the medical treatment of bacterial and viral infections.[34−40] In one example, Shikowitz and co-workers have used Photofrin for the PDT of recurrent respiratory papillomatosis by irradiation with a 630 nm laser light via endoscope to the infected location in throat or bronchus.[38−40] We hypothesized that the zanamivir component in compounds **4**−**6** might act as the specific

*To whom correspondence should be addressed. For Y.-S.E.C.: phone, 886-2-27871265; fax, 886-2-27899931; E-mail, ysecheng@gate.sinica.edu.tw. For J.-M.F.: phone, 8862-23637812; fax, 8862-23636359; E-mail: jmfang@ntu.edu.tw.

[a]Abbreviations: LANI, long-acting neuraminidase inhibitor; MDCK, Madin−Darby canine kidney; NA, neuraminidase; NAI, neuraminidase inhibitor; PDT, photodynamic therapy.

Published on Web 06/12/2009

Scheme 1. Synthesis of Zanamivir−Porphyrin Conjugate **4**

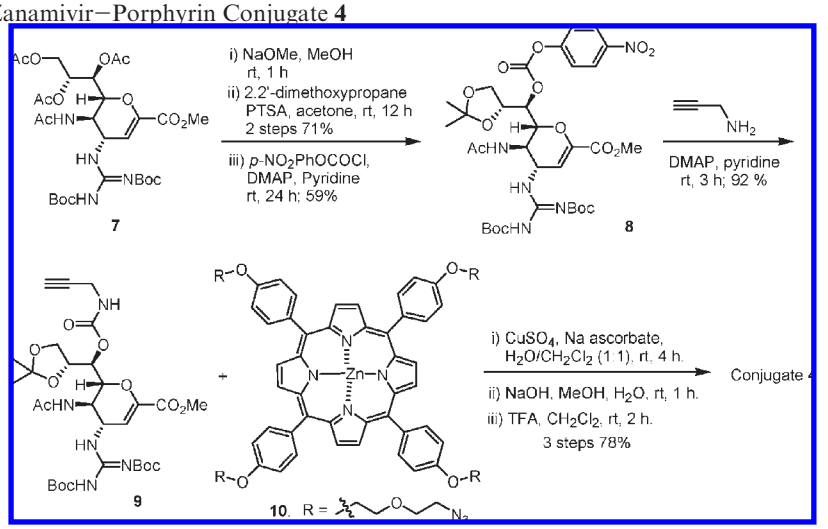

binders to influenza virus and the porphyrin component will act as a photosensitizer to generate singlet oxygen for inactivation of the attached viruses without harm to the host cells.

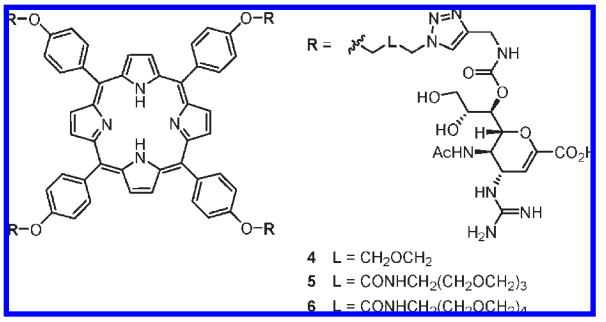

Results and Discussion

Chemistry. According to the previously reported method,[41,42] a zanamivir derivative (**7**) was prepared from sialic acid and activated as a *p*-nitrophenyl carbonate **8**, which was subsequently treated with propargylamine to afford the zanamivir derivative **9** with an alkynyl hinge (Scheme 1). On the other hand, the azide-annexed porphyrin derivative **10** was prepared by an S_N2 reaction of 5,10,15,20-tetrakis-(4-hydroxyphenyl)-21*H*,23*H*-porphine (**15a**) with 2-(2-azidoethoxy)ethyl methanesulfonate in the presence of a base K_2CO_3. The 1,3-dipolar addition (click reaction)[43,44] between the zanamivir derivative **9** and porphyrin **10** (as the zinc complex) was conducted in a mixed solvent of CH_2Cl_2/H_2O (1:1)[44] to give the desired zanamivir−porphyrin conjugate **4** in 78% overall yield after removal of the protecting groups.

In another approach, the click reactions of the zanamivir derivative **9** with the azido-linkers **11** and **12** were carried out, respectively, to give **13** and **14** (Scheme 2). The Fmoc groups in compounds **13** and **14** were removed, and the free amines were coupled with the carboxy-annexed porphyrin **15b** via amide bond formation to give the zanamivir−porphyrin conjugates **5** and **6** after removal of the protecting groups.

Biology. Zanamivir is a nanomolar inhibitor to most influenza neuraminidases that are tetrameric enzymes. The inhibitory activities of the zanamivir−porphyrin conjugates **4**−**6** were compared with zanamivir against two N1 neuraminidases from influenza viruses, A/WSN/1933 (H1N1)

Scheme 2. Synthesis of Zanamivir−Porphyrin Conjugates **5** and **6**

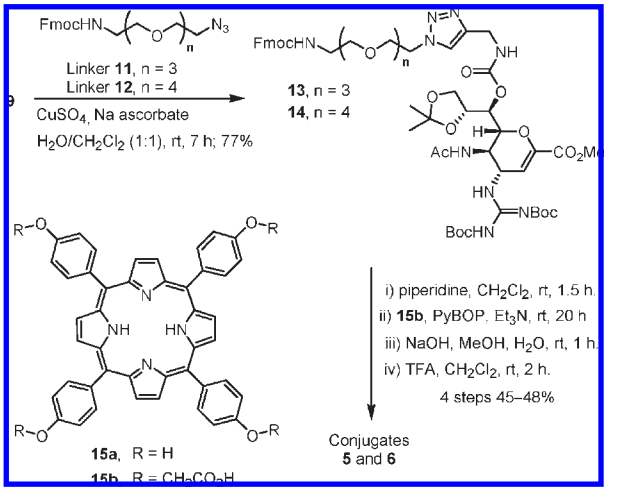

and A/Vietnam/1194/2003 (H5N1). A luminescence substrate of sialic acid 1,2-dioxetane derivative was used, in replacement of the fluorogenic substrate MUNANA, for the neuraminidase inhibitor (NAI) evaluations because the zanamivir conjugates contain a fluorescent moiety of porphyrin. To be sure that our assay is not biased against a single synthetic substrate, we also used fetuin as a "natural" substrate to compare the inhibitor activities against neuraminidase by measurement of the quantities of the cleavage product, sialic acid, in the presence of NAI. Under the assay conditions, we found that zanamivir at 10 nM resulted in 77% inhibition of the neuraminidase reaction, while at 40 nM, 88% inhibition resulted. In contrast, conjugate **4** at 10 and 40 nM resulted in less inhibition at 24% and 51% of the control values. All three zanamivir conjugates are nanomolar inhibitors, but they are somewhat less potent than zanamivir. Improved inhibitory activities resulted by increasing the spacer length in the conjugate. The conjugate **6** acted best, with IC_{50} values of 3.7−19 and 7.6 nM for neuraminidase inhibition of H1N1 and H5N1 viruses, respectively (Table 1).

The zanamivir−porphyrin conjugates and zanamivir were evaluated in their anti-influenza activities using cytopathic prevention assays. In contrast to the reduced potency than

Table 1. Comparison of Neuraminidase Inhibitory and Anti-influenza Activities of Zanamivir and the Porphyrin Conjugates

	NA inhibition IC_{50} (nM)[a]		anti-influenza EC_{50} (nM)[a]	
inhibitor	H1N1[b]	H5N1[c]	H1N1[b]	H5N1[c]
zanamivir (**1**)	2.4−4.0 (3)	2.5	11−27 (9)	613
conjugate **4**	11	ND[d]	2−8 (3)	11
conjugate **5**	8.5−38 (3)	16	0.5−4.2 (4)	ND[d]
conjugate **6**	3.7−19 (3)	7.6	0.1−2.1 (4)	ND[d]

[a] IC_{50} and EC_{50} values were determined by nonparametric curve fitting of assay results, and the shown data are ranges of assay results with number of assays in parentheses. [b] The H1N1 virus used is A/WSN/1933 (H1N1). [c] The H5N1 virus used is the recombinant influenza RG14 with HA and NA genes from A/Vietnam/1194/2004 (H5N1). [d] Not determined.

zanamivir in NAI assay, all three zanamivir conjugates are significantly more potent as anti-influenza inhibitors than zanamivir. Using plaque yield reduction assay, the conjugate **4** showed about 55-fold greater potency than zanamivir against avian H5N1 viruses (Table 1). The conjugates **4**−**6** also exhibit higher anti-influenza activities against human H1N1 viruses over zanamivir.

In the course of our investigation, we noticed that the influenza titer determined in the presence of the zanamivir−porphyrin conjugate **6** was reduced significantly in a concentration-dependent manner. For example, the influenza titer was reduced to less than 20% of the control value when the absorption of WSN viruses to MDCK cells were conducted in the presence of conjugate **6** at 40 nM and greater than 95% of the influenza titer was undetectable at 200 nM of **6**. In contrast, the presence of zanamivir caused only partial reduction in infectious titers to about 60% of the control level and stayed constant even with zanamivir at micromolar levels (Figure 1).

The disparity between the neuraminidase inhibition and the influenza replication inhibition of zanamivir and the zanamivir−porphyrin conjugates suggests that in addition to the capability of neuraminidase inhibition the conjugates may exert other inhibitory activities against influenza viruses. Enhanced anti-influenza activities of dimeric and polymeric zanamivir inhibitors have been reported[26−30] even though they are generally less potent in inhibiting neuraminidase activities. The enhanced anti-influenza activities may be attributable to multivalent effects,[45−47] and the dimeric and polymeric zanamivir inhibitors may also promote aggregation of viruses by interviral cross-linking of neuraminidases subunits.[7] It is conceivable that these inhibitory mechanisms also contribute to the enhanced antiviral activities of the tetrameric zanamivir conjugates **4**−**6**.

The inhibition of the early influenza infection events by neuraminidase inhibitors has been reported previously.[48] However, the possibility of the conjugates **4**−**6** in inhibiting the bindings of viral hemagglutinin with the sialic receptor was ruled out. According to our preliminary study (data not shown), the tetrameric zanamivir−porphyrin conjugates neither inhibited the hemagglutination of chicken red blood cells nor reduced the binding affinity of avian influenza hemagglutinin to α-2,3-sialic acid galactosyl oligomers. We speculated that the excessive inhibition by zanamivir−porphyrin conjugates to influenza infectious tier could be attributable to the porphyrin moiety of these compounds.

Porphyrins have been widely used for the treatments of tumors using PDT procedures.[31−33] Activation of porphyrin by red light causes energy transfer for the production of singlet

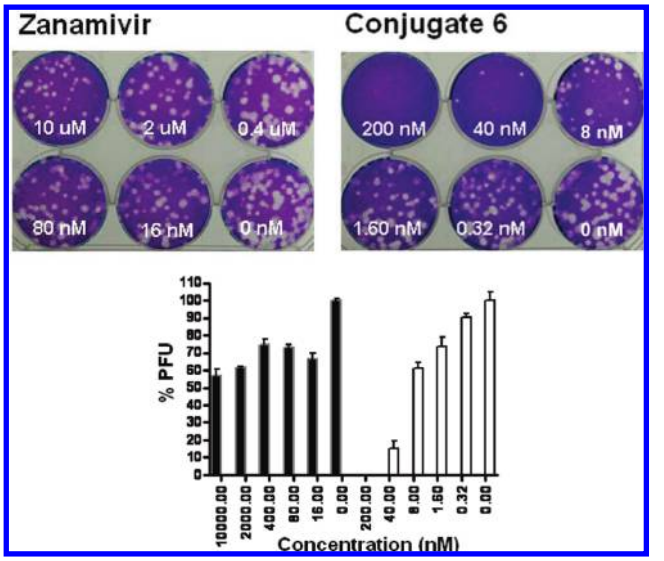

Figure 1. Reduction of influenza titers by zanamivir (filled bars) and the zanamivir−porphyrin conjugate **6** (open bars). WSN/33 virus samples in 6-well plates were treated during virus adsorption with zanamivir or conjugate **6** for 1 h at indicated concentrations. After adsorption, cells were washed twice with media, overlaid with 0.4% agarose, and incubated for 3 days. Plaques were visualized after fixation and staining of the cultures ($n = 4$).

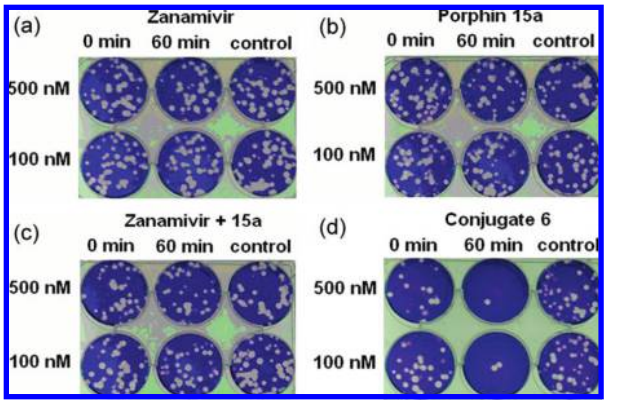

Figure 2. Light-induced influenza virus inactivation by zanamivir−porphyrin conjugate **6**. WSN/33 virus was incubated for 1 h with indicated concentration of compounds either in dark (0 min) or under a laminar flow hood light (~850 lx) for 60 min prior to adsorption to MDCK cells. The treated viral samples were diluted more than 1400-fold with medium and absorbed to MDCK cells. Control wells contained cells absorbed with light-treated viruses with conjugate **6** added at the end of the incubation before the 1400-fold dilution. After adsorption, cells were washed once with culture medium and overlaid with 0.4% agarose in culture medium. Plaques were visualized after incubation for 3 days.

oxygen and free radicals that are responsible to the destruction of tumors. To demonstrate that the porphyrin moiety in the zanamivir−porphyrin conjugates is effective for inactivation of influenza particles, we illuminated the viruses under laboratory light (~850 lx) in the presence of conjugate **6**. After a 1 h illumination, the presence of **6** at either 100 or 500 nM resulted in great influenza titer reductions (Figure 2d). In contrast, the presence of zanamivir or free porphyrin alone did not produce any detectable virus inactivation under the identical light treatments (Figure 2a,b). Even in the presence of both zanamivir and porphyrin at 100 or 500 nM, the light-induced influenza inactivation was not observed (Figure 2c).

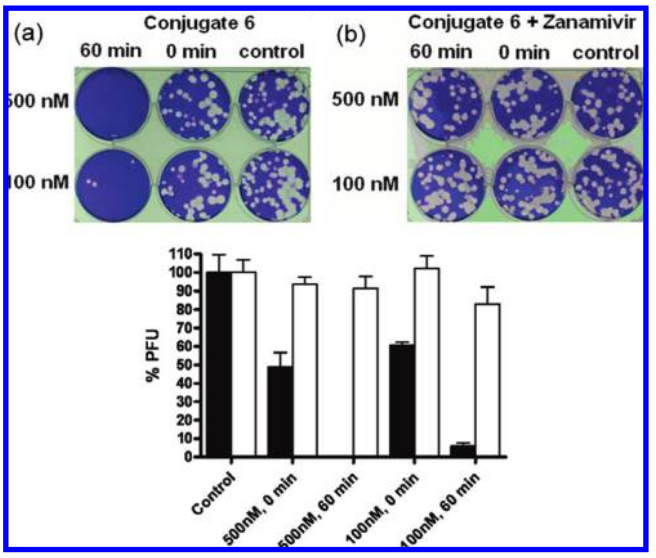

Figure 3. Neutralization of the conjugate **6** mediated influenza inactivation by excessive zanamivir. (a) WSN/33 viral samples ($n = 3$) were treated as described in Figure 2 (left top); (b) added with additional 10-fold excess zanamivir for absorption and viral plaque determinations. The resulting plaque number changes in the absence (filled bars) and presence of 10-fold excess zanamivir (open bars) are plotted as shown.

The results in Figure 2 led us to hypothesize that the viral inactivation by compound **6** was due to the local high concentration of the porphyrin conjugates brought to the viral surface by the high affinity of the zanamivir moieties to the viral membrane-bound neuraminidase. The high concentrations of **6** accumulated at close proximity to the viral surface could constitute the viral destructive effect under relatively low illumination conditions of laboratory lights. In contrast, free porphyrin at similar concentrations, both alone or in combination with zanamivir, could not be accumulated to high local concentrations at the viral surface and thus were ineffective in inactivating influenza viruses by light treatments. To test this hypothesis, we investigated if the presence of excessive zanamivir could compete out the conjugate **6** bound to the membrane neuraminidase, resulting in much lower local concentrations of **6** at the viral surface and neutralize the viral inactivation activities. Such an experiment was conducted, and the result obtained was exactly as predicted. Figure 3 shows that the influenza inactivation activities by conjugate **6** were greatly blocked in the presence of zanamivir at 10-fold excess. This result is consistent with the explanation that when free zanamivir competed out the molecules of **6** from influenza viral surfaces, the released molecules of **6** in solution would not cause viral inactivation.

Conclusion

We have prepared a novel class of tetrameric zanamivir conjugates **4**−**6** with a porphyrin core structure. These compounds in general are slightly less potent than zanamivir in neuraminidase inhibition but significantly more potent in inactivation of influenza viruses. The results of our study suggest that the enhanced anti-influenza activities of these bifunctional compounds could be due to the inhibition of viral neuraminidase and the physical inactivation of the virus infectivity. The local high concentration of porphyrin is attributable to the greater impact on viral inactivation. The molecules of zanamivir−porphyrin conjugates might be brought to the viral surface through the high affinity of the zanamivir moieties in a manner resembling the "magic bullet" mechanism.[49,50] Light sensitization of the porphyrin payload generates highly reactive singlet oxygen in close proximity, causing the inactivation of influenza viruses by directly targeting the viral neuraminidase.

We have shown a "magic bullet" approach to inactivate influenza viruses using in vitro assays. To demonstrate the efficacy of the zanamivir−porphyrin conjugate in an in vivo model, we would need to formulate the conjugate to a form compatible to delivery to the respiratory track of testing animals that are being treated by an illumination devise. For possible clinical application, we surmise that patients could be administered with the formulated conjugate by an inhalation device and later treated in a manner similar to photodynamic therapy[38−40] to reduce the viral loads that are often critical to the disease outcome.

Experimental Section

Materials and Methods. All the reagents and solvents were reagent grade and were used without further purification unless otherwise specified. All solvents were anhydrous grade unless indicated otherwise. CH_2Cl_2 was distilled from CaH_2. All nonaqueous reactions were carried out in oven-dried glassware under a slight positive pressure of argon unless otherwise noted. Reactions were magnetically stirred and monitored by thin-layer chromatography on silica gel using aqueous *p*-anisaldehyde as visualizing agent. Silica gel (0.040−0.063 mm particle sizes) and LiChroprep RP-18 (0.040−0.063 mm particle sizes) were used for column chromatography. Flash chromatography was performed on silica gel of 60−200 μm particle size. Molecular sieves were activated under high vacuum at 220 °C over 6 h.

Melting points were recorded on a Yanaco or Electrothermal MEL-TEMP 1101D apparatus in open capillaries and are not corrected. Optical rotations were measured on digital polarimeter of Japan JASCO Co. DIP-1000. $[\alpha]_D$ values are given in units of 10^{-1} deg cm^2 g^{-1}. Infrared (IR) spectra were recorded on Nicolet Magna 550-II or Thermo Nicolet 380 FT-IR spectrometers. UV−visible spectra were measured on a Perkin-Elmer Lambda 35 spectrophotometer. Nuclear magnetic resonance (NMR) spectra were obtained on Varian Unity Plus-400 (400 MHz) spectrometer. Chemical shifts (δ) are given in parts per million (ppm) relative to δ_H 7.26/δ_C 77.0 (central line of t) for $CHCl_3/CDCl_3$, δ_H 4.80 for H_2O/D_2O, δ_H 3.31/δ_C 48.2 for CD_3OD-d_4, or δ_H 2.49/δ_C 39.5 for DMSO-d_6. The splitting patterns are reported as s (singlet), d (doublet), t (triplet), q (quartet), m (multiplet), dd (double of doublets), and br (broad). Coupling constants (J) are given in Hz. Distortionless enhancement polarization transfer (DEPT) spectra were taken to determine the types of carbon signals. The ESI-MS experiments were conducted on a Bruker Daltonics BioTOF III high-resolution mass spectrometer.

Purity of compounds tested on influenza virus was assessed to be ≥95% by HPLC (Agilent HP-1100) with detection at 423 nm wavelength.

Influenza A/WSN/1933 (H1N1) (from Dr. Shin-Ru Shih, Chang Gung University, Taiwan) was cultured in the allantoic cavities of 10-day-old embryonated chicken eggs for 72 h and purified by sucrose gradient centrifugation. Madin−Darby canine kidney (MDCK) cells were obtained from the American Type Culture Collection (Manassas, VA), and were grown in DMEM (Dulbecco's modified Eagle medium, GibcoBRL) containing 10% fetal bovine serum (GibcoBRL) and penicillin−streptomycin (GibcoBRL) at 37 °C under 5% CO_2.

Synthetic Procedures. Zanamivir (Relenza, **1**),[41] compounds **7**[42] and **8**[42] were prepared according to the previously described methods.

Compound 9. To a solution of carbonate **8** (500 mg, 0.66 mmol) in pyridine (7 mL) was added propargylamine (0.064 mL, 1.0 mmol) and DMAP (122 mg, 1.0 mmol). The mixture was stirred at room temperature for 3 h and then concentrated under reduced pressure. The residue was partitioned with EtOAc and 1 M HCl. The organic layer was washed with saturated $NaHCO_3$ and brine, dried over $MgSO_4$, filtered, and concentrated by rotary evaporation under reduced pressure. The crude material was purified by silica gel column chromatography (EtOAc/hexane = 2:3) to yield carbamate **9** (408 mg, 92%). $C_{30}H_{45}N_5O_{12}$; white solid, mp 138−139 °C. TLC (EtOAc/hexane = 1:1) R_f = 0.29; $[\alpha]^{19}_D$ +44.4 (*c* 0.37, EtOAc). IR ν_{max} (neat) 3311, 2980, 2930, 1730, 1642, 1611, 1249, 1142, 1056 cm^{-1}. ^1H NMR (400 MHz, $CDCl_3$) δ 11.29 (1 H, s), 8.35 (1 H, d, *J* = 8.4 Hz), 6.50 (1 H, d, *J* = 9.6 Hz), 5.82 (1 H, d, *J* = 2.4 Hz), 5.26 (1 H, br s), 5.20 (1 H, br s), 5.12−5.07 (1 H, m), 4.33−4.30 (1 H, m), 4.28−4.05 (2 H, m), 4.00−3.94 (2 H, m), 3.81−3.76 (1 H, m), 3.73 (3 H, s), 2.21 (1 H, s), 2.68 (1 H, br), 1.85 (3 H, s), 1.42 (18 H, s), 1.33 (3 H, s), 1.29 (3 H, s). ^{13}C NMR (100 MHz, $CDCl_3$) 170.6, 162.6, 161.6, 156.6, 154.9, 152.4, 144.7, 109.9, 108.7, 83.6, 79.5, 77.4, 77.2, 74.7, 71.6, 70.1, 65.7, 52.3, 49.0, 47.7, 31.1, 28.2 (3×), 28.0 (3×), 26.5, 25.4, 23.0, ESI-HRMS calcd for $C_{30}H_{46}N_5O_{12}$: 668.3143; found: *m*/*z* 668.3140 $[M + H]^+$.

Compound 10. According to the reported procedure,[51] 2-(2-azidoethoxy)ethyl methanesulfonate (90 mg, 0.43 mmol) was prepared and treated with a solution of 5,10,15,20-tetrakis-(4-hydroxyphenyl)-21*H*,23*H*-porphine (61 mg, 0.09 mmol, commercially available) in DMF in the presence of K_2CO_3 (124 mg, 0.9 mmol). The mixture was stirred at 100 °C for 3 h, $ZnCl_2$ (122 mg, 0.9 mmol) was added, and it was stirred at 100 °C for another 3 h. After concentration by rotary evaporation under reduced pressure, the residue was dissolved in CH_2Cl_2, washed with H_2O and brine, dried over $MgSO_4$, and concentrated. The residue was purified on a silica gel column by elution with CH_2Cl_2 to give the porphyrin−zinc complex **10** (88 mg, 82%). $C_{60}H_{56}N_{16}O_8Zn$; purple solid, mp 162−163 °C. TLC (CH_2Cl_2) R_f = 0.65. UV−vis (DMSO) λ_{max} (log ε) 604 (4.1), 563 (4.2), 431 (5.7), 410 (4.6) nm. IR ν_{max} (neat) 2101 (azido), 1245, 1176, 995 cm^{-1}. ^1H NMR (400 MHz, $CDCl_3$) δ 8.94 (8 H, s), 8.09 (8 H, d, *J* = 8.0 Hz), 7.21 (8 H, d, *J* = 8.0 Hz), 4.23 (8 H, t, *J* = 4.8 Hz), 3.81 (8 H, t, *J* = 4.8 Hz), 3.53 (8 H, t, *J* = 4.8 Hz), 3.11 (8 H, t, *J* = 4.8 Hz). ^{13}C NMR (100 MHz, $CDCl_3$) 158.1 (4×), 150.2 (8×), 135.5 (4×), 135.2 (8×), 131.7 (8×), 120.5 (4×), 112.6 (8×), 70.1 (4×), 69.8 (4×), 67.6 (4×), 50.5 (4×). ESI-HRMS calcd for $C_{60}H_{57}N_{16}O_8Zn$: 1193.3837; found: *m*/*z* 1193.3846 $[M + H]^+$.

1-(Fmoc-amino)-11-azido-3,6,9-trioxaundecane (Linker 11). Staudinger reaction of 1,11-diazido-3,6,9-trioxaundecane (commercially available) with 0.95 equiv of PPh_3, according to a procedure similar to that for linker **12**, gave 1-amino-11-azido-3,6,9-trioxaundecane (777 mg, 3.56 mmol), which reacted with fluorenylmethyloxycarbonyl chloride (FmocCl, 1.02 g, 3.92 mmol) in the presence of $NaHCO_3$ to give the linker **11** (1.3 g, 83%). $C_{23}H_{28}N_4O_5$; pale-yellow oil. TLC (EtOAc/hexane = 2:1) R_f = 0.54. IR ν_{max} (neat) 2922, 2103, 1715 cm^{-1}. ^1H NMR (400 MHz, $CDCl_3$) δ 7.74 (2 H, d, *J* = 7.6 Hz), 7.58 (2 H, d, *J* = 7.6 Hz), 7.38 (2 H, dd, *J* = 7.6, 7.2 Hz), 7.29 (2 H, dd, *J* = 7.6, 7.2 Hz), 5.39 (1 H, br s), 4.40 (2 H, d, *J* = 6.8 Hz), 4.21 (1 H, t, *J* = 6.8 Hz), 3.60 (10 H, m), 3.56 (2 H, m), 3.39 (2 H, m), 3.34 (2 H, m). ^{13}C NMR (100 MHz, $CDCl_3$) δ 156.3, 143.8 (2×), 141.1 (2×), 127.5 (2×), 126.8 (2×), 124.9 (2×), 119.8 (2×), 70.6 (2×), 70.5, 70.3, 70.0 (2×), 66.5, 50.6, 47.3, 40.9. ESI-HRMS calcd for $C_{23}H_{29}N_4O_5$: 441.2138; found: *m*/*z* 441.2138 $[M + H]^+$.

1-(Fmoc-amino)-14-azido-3,6,9,12-tetraoxatetradecane (Linker 12). To a solution of 1,14-diazido-3,6,9,12-tetraoxatetradecane[52] (950 mg, 3.3 mmol, commercially available) in EtOAc (2 mL) and Et_2O (2 mL) was added 2 M HCl (3.3 mL) and PPh_3 (812 mg, 3.1 mmol). The mixture was stirred at room temperature for 24 h. The aqueous layer was washed with CH_2Cl_2 (3×), and the organic phase was discarded. The solution was basified with $KOH_{(aq)}$ and extracted with CH_2Cl_2 (5×). The combined organic phase was dried over $MgSO_4$, filtered, and concentrated in vacuo to give 1-amino-14-azido-3,6,9,12-tetraoxatetradecane (650 mg, 80%). $C_{10}H_{22}N_4O_4$; oil. ^1H NMR (400 MHz, $CDCl_3$) δ 3.66−3.61 (16 H, m), 3.48 (2 H, t, *J* = 5.2 Hz), 3.37 (2 H, t, *J* = 5.2 Hz), 2.84 (2 H, br). ^{13}C NMR (100 MHz, $CDCl_3$) δ 73.5, 70.7 (2×), 70.6 (3×), 70.3, 70.0, 50.8, 42.0.

To a solution of 1-amino-14-azido-3,6,9,12-tetraoxatetradecane (650 mg, 2.48 mmol) in 1,4-dioxane (10 mL) was added 1.8 M $NaHCO_3$ (3 mL). The solution was cooled in ice-bath, and a solution of FmocCl (707 mg, 2.73 mmol) in 1,4-dioxane (10 mL) was added dropwise. The mixture was stirred at room temperature for 8 h, and then partitioned with CH_2Cl_2 and H_2O. The organic layer was dried over $MgSO_4$, concentrated by rotary evaporation under reduced pressure. The residue was purified by silica gel column chromatography (EtOAc/hexane = 1:1) to give the linker **12** (865 mg, 72%). $C_{25}H_{32}N_4O_6$; pale-yellow oil. TLC (EtOAc) R_f = 0.61. IR ν_{max} (neat) 2921, 2100, 1712 cm^{-1}. ^1H NMR (400 MHz, $CDCl_3$) δ 7.74 (2 H, d, *J* = 7.6 Hz), 7.59 (2 H, d, *J* = 7.6 Hz), 7.38 (2 H, dd, *J* = 7.6, 7.2 Hz), 7.29 (2 H, dd, *J* = 7.6, 7.2 Hz), 5.55 (1 H, br), 4.39 (2 H, d, *J* = 7.2 Hz), 4.21 (1 H, t, *J* = 7.2 Hz), 3.64−3.60 (14 H, m), 3.56 (2 H, m), 3.39 (2 H, m), 3.34 (2 H, m). ^{13}C NMR (100 MHz, $CDCl_3$) δ 156.4, 143.8 (2×), 141.1 (2×), 127.5 (2×), 126.9 (2×), 125.0 (2×), 119.8 (2×), 70.6 (2×), 70.5 (2×), 70.3 (2×), 70.1, 70.0, 66.5, 50.7, 47.3, 41.0. ESI-HRMS calcd for $C_{25}H_{33}N_4O_6$: 485.2400; found: *m*/*z* 485.2401 $[M + H]^+$.

Triazole Compound 13. To a solution of propargyl carbamate **9** (514 mg, 0.77 mmol) and the azido linker **11** (327 mg, 0.77 mmol) in CH_2Cl_2 (8 mL) and H_2O (8 mL) were added $CuSO_4 \cdot 5H_2O$ (58 mg, 0.23 mmol) and sodium ascorbate (137 mg, 0.69 mmol). The mixture was stirred at room temperature for 7 h and then partitioned with CH_2Cl_2 and H_2O. The organic layer was dried over $MgSO_4$, concentrated, and purified by silica gel column chromatography (CH_2Cl_2/MeOH = 25:1) to give a triazole product **13** (665 mg, 78%). $C_{53}H_{73}N_9O_{17}$; colorless solid, mp 84−86 °C. TLC (CH_2Cl_2/MeOH = 15:1) R_f = 0.23; $[\alpha]^{22}_D$ +11.26 (*c* 2.0, EtOAc). IR ν_{max} (neat) 2931, 1730, 1639, 1610, 1536, 1248, 1140 cm^{-1}. ^1H NMR (400 MHz, $CDCl_3$) δ 11.34 (1 H, s), 8.37 (1 H, d, *J* = 8.4 Hz), 7.82 (1 H, s), 7.69 (2 H, d, *J* = 7.6 Hz), 7.55 (2 H, d, *J* = 7.6 Hz), 7.33 (2 H, dd, *J* = 7.6, 7.2 Hz), 7.24 (2 H, dd, *J* = 7.6, 7.2 Hz), 6.60 (1 H, br s), 5.84 (1 H, s), 5.68 (2 H, br s), 5.21−5.13 (2 H, m), 4.41−4.26 (8 H, m), 4.18−3.94 (4 H, m), 3.76 (2 H, br), 3.72 (3 H, s), 3.54−3.51 (10 H, m), 3.33−3.32 (2 H, m), 1.87 (3 H, s), 1.44 (9 H, s), 1.43 (9 H, s), 1.28 (6 H, s). ^{13}C NMR (100 MHz, $CDCl_3$) δ 170.5, 162.2, 161.6, 156.6, 156.3, 155.3, 152.4, 144.7 (2×), 143.7 (2×), 141.0 (2×), 127.4 (2×), 126.8 (2×), 124.8 (2×), 123.2, 119.7 (2×), 109.8, 108.6, 83.4, 79.5, 74.6, 70.3 (2×), 70.2 (2×), 70.1 (2×), 69.9, 69.1, 66.3, 65.7, 52.3, 50.0, 49.0, 47.9, 47.2, 40.8, 36.9, 28.2 (3×), 28.0 (3×), 26.5, 25.3, 23.0. ESI-HRMS calcd for $C_{53}H_{74}N_9O_{17}$: 1108.5203; found: *m*/*z* 1108.5197 $[M + H]^+$.

Triazole Compound 14. To a solution of propargyl carbamate **9** (267 mg, 0.4 mmol) and the azido linker **12** (194 mg, 0.4 mmol) in CH_2Cl_2 (4 mL) and H_2O (4 mL) was added $CuSO_4 \cdot 5H_2O$ (30 mg, 0.12 mmol) and sodium ascorbate (71 mg, 0.36 mmol). The mixture was stirred at room temperature for 7 h and then partitioned with CH_2Cl_2 and H_2O. The organic layer was dried over $MgSO_4$, concentrated, and purified by silica gel column chromatography (CH_2Cl_2/MeOH = 30:1) to give a triazole product **14** (355 mg, 77%). $C_{55}H_{77}N_9O_{18}$; colorless solid, mp 77−79 °C. TLC (CH_2Cl_2/MeOH = 30:1) R_f = 0.16; $[\alpha]^{22}_D$ +6.78 (*c* 1.5, EtOAc). IR ν_{max} (neat) 2925, 1731, 1637, 1610, 1540, 1249, 1140 cm^{-1}. ^1H NMR (400 MHz, $CDCl_3$) δ 11.38 (1 H, s), 8.40 (1 H, d, *J* = 8.4 Hz), 7.84 (1 H, br s), 7.71 (2 H, d, *J* = 7.6 Hz), 7.56 (2 H, d, *J* = 7.2 Hz), 7.34 (2 H, dd, *J* = 7.2, 7.2 Hz), 7.26 (2 H, dd, *J* = 7.6, 7.2 Hz), 6.24 (1 H, d, *J* = 7.6 Hz), 5.85 (1 H, d, *J* = 2.0 Hz), 5.67−5.62 (2 H, m), 5.21−5.16 (2 H, m), 4.44−4.28 (8 H, m), 4.19−3.98 (4 H, m), 3.79 (2 H, s), 3.73 (3 H, s), 3.58−3.52 (14 H, m), 3.56−3.32 (2 H, m), 1.88 (3 H, s), 1.45 (9 H, s), 1.44

(9 H, s), 1.40 (6 H, s). ^{13}C NMR (100 MHz, $CDCl_3$) δ 170.5, 162.7, 161.6, 156.6, 156.3, 155.3, 152.4, 144.8, 144.7, 143.7 (2×), 141.0 (2×), 127.4 (2×), 126.8 (2×), 124.9 (2×), 123.2, 119.7 (2×), 109.7, 108.7, 83.5, 79.5, 77.2, 74.6, 70.4 (2×), 70.3 (2×), 70.2 (2×), 70.1, 70.0, 69.2, 66.4, 65.8, 52.3, 50.1, 48.9, 48.2, 47.2, 40.9, 37.0, 28.3 (3×), 28.0 (3×), 26.5, 25.4, 23.1. ESI-HRMS calcd for $C_{55}H_{78}N_9O_{18}$: 1152.5459; found: m/z 1152.5463 $[M + H]^+$.

Zanamivir−Porphyrin Conjugate 4. To a solution of propargyl carbamate **9** (42.7 mg, 0.064 mmol) and the azido-linked porphin−zinc complex **10** (17.4 mg, 0.015 mmol) in CH_2Cl_2 (0.5 mL) and H_2O (0.5 mL) were added $CuSO_4 \cdot 5H_2O$ (2.5 mg, 0.01 mmol) and sodium ascorbate (5.94 mg, 0.03 mmol). The mixture was stirred at room temperature for 4 h and then partitioned with CH_2Cl_2 and H_2O. The organic layer was dried over $MgSO_4$, concentrated, and chromatographed on a LH-20 column by elution with MeOH to give the desired triazole product (56.5 mg, 98%). $C_{180}H_{236}N_{36}O_{56}Zn$; purple solid; mp > 240 °C (decomposed). TLC (CH_2Cl_2/MeOH = 9:2) R_f = 0.58. UV−vis (DMSO) λ_{max} (log ε) 604 (4.4), 563 (4.5), 431 (5.8), 410 (4.75) nm. IR ν_{max} (neat) 3241, 1730, 1645, 1610, 1250, 1144, 1058 cm^{-1}. ^{1}H NMR (400 MHz, $CDCl_3$) δ 11.36 (4 H, s), 8.87 (8 H, s), 8.39 (4 H, d, J = 8.0 Hz), 8.11 (8 H, d, J = 8.0 Hz), 7.73 (4 H, s), 7.21 (8 H, d, J = 8.0 Hz), 6.25 (4 H, d, J = 8.8 Hz), 5.84 (4 H, s), 5.12−5.08 (12 H, m), 4.37−3.71 (72 H, m), 1.85 (12 H, s), 1.45 (36 H, s), 1.42 (36 H, s), 1.15 (12 H, s), 1.12 (12 H, s). ^{13}C NMR (100 MHz, $CDCl_3$) δ 170.4 (4×), 162.8 (8×), 161.6 (4×), 157.8 (4×), 156.6 (8×), 155.2 (4×), 152.4 (4×), 150.1 (4×), 144.8 (4×), 144.3 (4×), 136.0 (4×), 135.4 (8×), 131.4 (8×), 123.2 (4×), 120.1 (4×), 112.4 (4×), 109.7 (4×), 108.6 (8×), 83.5 (4×), 79.5 (4×), 77.2 (4×), 74.4 (4×), 69.8 (4×), 69.4 (4×), 67.5 (4×), 65.7 (4×), 52.4 (4×), 50.2 (4×), 49.0 (4×), 48.1 (4×), 36.3 (4×), 28.3 (12×), 28.1 (12×), 26.4 (4×), 25.3 (4×), 23.2 (4×). ESI-HRMS calcd for $[C_{180}H_{239}N_{36}O_{56}Zn]^{3+}$ 1289.2095, $[C_{180}H_{240}N_{36}O_{56}Zn]^{4+}$ 967.1590; found: m/z 1289.1978 $[M+3H]^{3+}$, 967.1675 $[M+4H]^{4+}$.

To the above-prepared triazole compound (30 mg) in MeOH (2 mL) was added 1 M NaOH (0.5 mL) and stirred at room temperature for 0.5 h. The mixture was neutralized by addition of resin Dowex 50W × 8 (H^+), filtered, and concentrated by rotary evaporation under reduced pressure. The residue was dissolved in CH_2Cl_2 (1 mL) and stirred with TFA (1 mL) at room temperature for 3 h. The mixture was concentrated by rotary evaporation under reduced pressure. The residue was triturated with Et_2O, and the product **4** (as the TFA salt, 20 mg, 80%) was separated by Sephadex G−25 (eluent: 0.1% TFA in H_2O). The purity of the product **4** was >95% as shown by HPLC on a ZORBAX 300SB-C18 column (9.4 mm × 250 mm, 5 μm), t_R = 9.61 min (solvent A: 90% acetonitrile containing 0.1% TFA; solvent B: 2% acetonitrile containing 0.1% TFA, gradient 60−100%A in 40 min) $C_{132}H_{154}F_{12}N_{36}O_{48}$; green solid, mp > 170 °C (decomposed). UV−vis (DMSO) λ_{max} (log ε) 651 (3.9), 594 (3.9), 557 (4.3), 519 (4.4), 424 (5.7) nm. IR ν_{max} (neat) 3385, 1673, 1601 cm^{-1}. ^{1}H NMR (400 MHz, CD_3OD) δ 8.73 (8 H, s), 8.59 (8 H, d, J = 7.2 Hz), 8.12 (4 H, s), 7.66 (8 H, d, J = 7.2 Hz), 5.88 (4 H, d, J = 2.0 Hz), 5.05 (4 H, d, 9.2 Hz), 4.72 (4 H, s), 4.60 (4 H, d, J = 9.2 Hz), 4.49−4.40 (16 H, m), 4.36−4.30 (4 H, m), 421−4.14 (12 H, m), 4.06−4.00 (12 H, m), 3.83−3.73 (4 H, m), 3.66−3.63 (4 H, m), 3.53−3.49 (4 H, m), 1.96 (12 H, s). ESI-HRMS calcd for $[C_{124}H_{153}N_{36}O_{40}]^{3+}$ 929.0352, $[C_{124}H_{154}N_{36}O_{40}]^{4+}$ 697.0282, $[C_{124}H_{155}N_{36}O_{40}]^{5+}$ 557.8240; found: m/z 929.0344 $[M+3H]^{3+}$, 697.0273 $[M+4H]^{4+}$, 557.8239 $[M+5H]^{5+}$.

Zanamivir−Porphyrin Conjugate 5. A solution of compound **13** (617 mg, 0.557 mmol) in CH_2Cl_2 (8 mL) was treated with piperidine (2 mL) at room temperature for 1.5 h, concentrated, and purified by silica gel column chromatography (CH_2Cl_2/MeOH = 15:1) to give the desired amine (380 mg, 77%). The amine (380 mg, 0.429 mmol) was stirred with 5,10,15,20-tetrakis (4-carboxymethoxyphenyl)-21*H*,23*H*-porphine (**15b**, 88.8 mg, 0.097 mmol, commercially available) in the presence of PyBOP (262 mg, 0.50 mmol) and Et_3N (0.27 mL, 1.94 mmol) in DMF (4 mL) at room temperature for 20 h. After concentration by rotary evaporation under reduced pressure, the residue was dissolved in CH_2Cl_2 and washed with saturated $NaHCO_3$ and brine. The organic layer was dried over $MgSO_4$, concentrated by rotary evaporation under reduced pressure, and purified by LH-20 column chromatography with elution of MeOH to give the desired coupling product (255 mg, 60%).

The above-prepared coupling product (145 mg, 0.033 mmol) in THF (2 mL) was added 1 M $NaOH_{(aq)}$ (2 mL) and stirred at room temperature for 0.5 h. The mixture was neutralized by addition of resin Dowex 50W × 8 (H^+), filtered, and concentrated by rotary evaporation under reduced pressure. The residue was dissolved in CH_2Cl_2 (3 mL) and stirred with TFA (3 mL) at room temperature for 3 h. The mixture was concentrated by rotary evaporation under reduced pressure. The residue was triturated with Et_2O, and the product **5** (as the TFA salt, 120 mg, 92%) was separated on a Sephadex G−25 column (eluent: 0.1% TFA in H_2O).

Coupling product: $C_{204}H_{282}N_{40}O_{68}$; solid, mp 126−128 °C. UV−Vis (DMSO) λ_{max} (log ε) 651 (3.86), 594 (3.78), 556 (4.14), 518 (4.27), 423 (5.71) nm. IR ν_{max} (neat) 2929, 1731, 1642, 1610, 1246, 1141 cm^{-1}. ^{1}H NMR (400 MHz, $CDCl_3$ + CD_3CN, a mixture of rotamers) δ 11.34 (4 H, s), 8.80−8.78 (8 H, m), 8.36 (4 H, d, J = 8.0 Hz), 8.10−8.04 (8 H, m), 7.88−7.84 (4 H, m), 7.36 (4 H, br), 7.28−7.25 (8 H, m), 6.51 (5 H, br), 5.85 (4 H, d, J = 2.0 Hz), 5.81 (0.6 H, br), 5.67 (2.4 H, br), 5.23−5.10 (8 H, m), 4.94−4.75 (8 H, m), 4.44−3.50 (104 H, m), 1.87 (12 H, s), 1.40 (72 H, s), 1.31−1.18 (24 H, m), −2.84 (2 H, s). ^{13}C NMR (100 MHz, $CDCl_3$ + CD_3CN) δ 170.4 (4×), 167.9 (4×), 165.7 (4×), 162.6 (8×), 161.5 (4×), 156.8 (4×), 156.3 (8×), 155.2 (4×), 152.2 (4×), 144.6 (4×), 144.3 (4×), 135.3 (8×), 135.2 (8×), 130.5 (4×), 123.0 (4×), 123.0 (4×), 112.8 (4×), 112.7 (4×), 109.9 (4×), 108.4 (8×), 83.2 (4×), 79.2 (4×), 77.2 (4×), 74.6 (4×), 70.2 (8×), 70.0 (4×), 69.6 (4×), 69.5 (4×), 69.0 (4×), 67.4 (4×), 65.5 (4×), 52.21 (4×), 49.8 (4×), 48.9 (4×), 47.5 (4×), 38.7 (4×), 28.0 (12×), 27.8 (12×), 26.2 (4×), 25.2 (4×), 22.8 (4×). ESI-HRMS calcd for $[C_{204}H_{291}N_{40}O_{68}]^{3+}$ 1460.6633; found: m/z 1460.6589 $[M + 3 H]^{3+}$.

Zanamivir−porphyrin conjugate **5**: >95% purity by HPLC, t_R = 12.12 min (gradient 30−70% A in 40 min); green solid, mp > 130 °C (decomposed). UV−vis (DMSO) λ_{max} (log ε) 651 (3.67), 594 (3.58), 556 (3.98), 518 (4.11), 423 (5.57) nm. IR ν_{max} (neat) 3423, 1647 cm^{-1}. ^{1}H NMR (400 MHz, CD_3OD) δ 8.73 (8 H, s), 8.60−8.57 (8 H, m), 7.99 (4 H, s), 7.72−7.67 (8 H, m), 5.87/5.74 (4 H, s), 5.23/5.17 (4 H, s), 5.01 (4 H, d, J = 8.8 Hz), 4.95 (8 H, s), 4.60−4.55 (12 H, m), 4.42−4.16 (16 H, m), 3.99−3.45 (64 H, m), 1.94/1.80 (12 H, s). MALDI-HRMS calcd for $[C_{148}H_{195}N_{40}O_{52}]^+$ 3365.388; found: m/z 3365.431 $[M + H]^+$.

Zanamivir−Porphyrin Conjugate 6. By a procedure similar to that for compound **5**, the Fmoc group in **14** (450 mg, 0.39 mmol) was removed by piperidine and the free amine (300 mg, 0.32 mmol) was reacted with **15b** (66.8 mg, 0.073 mmol) in the presence of PyBOP (197 mg, 0.38 mmol) and Et_3N (0.2 mL, 1.46 mmol) to give the coupling product (186 mg, 56%), which was converted to the desired zanamivir−phorphyrin conjugate **6** (186 mg, 56%) by sequential saponification (1 M NaOH, room temperature, 1 h) and acid treatment (TFA, room temperature, 1 h) to remove the protecting groups.

Coupling product: $C_{212}H_{298}N_{40}O_{72}$; purple solid; mp 122−124 °C. UV−Vis (DMSO) λ_{max} (log ε) 651 (3.75), 593 (3.65), 556 (4.05), 519 (4.18), 423 (5.63) nm. IR ν_{max} (neat) 2928, 1732, 1646, 1610, 1248, 1139 cm^{-1}. ^{1}H NMR (400 MHz, $CDCl_3$ + CD_3CN) (a mixture of rotamers) δ 11.32 (4 H, s), 8.78−8.76 (8 H, m), 8.31 (4 H, d, J = 8.4 Hz), 8.07−8.02 (8 H, m), 7.83−7.80 (5 H, m), 7.42 (3 H, br), 7.27−7.24 (8 H, m), 6.89−6.67 (5 H, br), 5.83−5.72 (7 H, m), 5.22−5.04 (8 H, m), 4.91−4.74 (8 H, m), 4.38−3.50 (120 H, m), 1.84 (12 H, s), 1.39−1.37 (72 H, m), 1.25 (24 H, m), −2.87 (2 H, s). ^{13}C NMR (100 MHz, $CDCl_3$ + CD_3CN) δ 170.4 (4×), 167.9 (4×), 165.7 (4×), 162.7 (8×), 161.5 (4×), 156.8 (4×), 156.4 (8×), 155.3 (4×), 152.2 (4×), 144.7 (4×), 144.5 (4×), 135.3 (8×), 135.2 (8×), 130.6 (4×), 123.1 (4×), 119.1 (4×), 112.8 (4×), 112.7 (4×), 109.9 (4×), 108.5 (8×), 83.2 (4×), 79.2 (4×),

77.2 (4×), 74.6 (4×), 70.3 (8×), 70.2 (4×), 70.1 (8×), 69.7 (4×), 69.5 (4×), 69.1 (4×), 67.5 (4×), 65.6 (4×), 52.2 (4×), 49.9 (4×), 49.0 (4×), 47.7 (4×), 38.8 (4×), 28.1 (12×), 27.9 (12×), 26.4 (4×), 25.5 (4×), 22.9 (4×). ESI-HRMS calcd for $[C_{212}H_{301}N_{40}O_{72}]^{3+}$ 1519.3649; found: m/z 1519.3816 $[M + 3\ H]^{3+}$.

Zanamivir−porphyrin conjugate **6**: >95% purity by HPLC, t_R = 11.25 min (gradient 30−70% A in 40 min); green powder; mp >120 °C (decomposed). UV−vis (DMSO) λ_{max} (log ε) 651 (3.80), 594 (3.71), 556 (4.10), 518 (4.23), 423 (5.67) nm. IR ν_{max} (neat) 3407, 1672 cm^{-1}. ^1H NMR (400 MHz, CD_3OD) δ 8.73 (8 H, s), 8.61−8.57 (8 H, m), 7.99−7.73 (4 H, m), 7.70−7.67 (8 H, m), 5.87/5.76 (4 H, s), 5.23/5.15 (4 H, s), 5.03 (4 H, d, J=8.8 Hz), 4.95 (8 H, s), 4.65−4.29 (24 H, m), 4.20−4.15 (4 H, m), 4.00−3.84 (12 H, m), 3.76−3.46 (56 H, m), 1.96/1.80 (12 H, s). ESI-HRMS calcd for $[C_{156}H_{215}N_{40}O_{56}]^{5+}$ 709.3047; found: m/z 709.3077 $[M + 5\ H]^{5+}$.

Determination of Influenza Virus $TCID_{50}$. The $TCID_{50}$ (50% tissue culture infectious dose) was determined by serial dilution of the influenza virus stock onto 100 μL MDCK cells at 1×10^5 cells/mL in 96-well microplates. The infected cells were incubated at 37 °C under 5.0% CO_2 for 48 h and added to each wells with 100 μL per well of CellTiter 96 AQueous Non-Radioactive Cell Proliferation Assay reagent (Promega). After incubation at 37 °C for 15 min, absorbance at 490 nm was read on a plate reader. Influenza virus $TCID_{50}$ was determined using Reed−Muench method.[53,54]

Determination of NA Activity by a Fluorescent Assay. The neuraminidase activity was measured using diluted allantoic fluid harvest from influenza A/WSN/1933 (H1N1) infected embryonated eggs. A fluorometric assay was used to determine the NA activity with the fluorogenic substrate 2′-(4-methylumbelliferyl)-α-D-*N*-acetylneuraminic acid (MUNANA; Sigma). The fluorescence of the released 4-methylumbelliferone was measured in Envision plate reader (Perkin-Elmer, Wellesley, MA) using excitation and emission wavelengths of 365 and 460 nm, respectively. Neuraminidase activity was determined at 200 μM of MUNANA. Enzyme activity was expressed as the fluorescence increase during 15 min incubation at room temperature.

Determination of NA Activity by a Chemiluminescent Assay. The neuraminidase was measured using virus-associated neuraminidase activities. NA activity was determined by a commercially available kit that uses a 1,2-dioxetane derivative of sialic acid (NA-STAR) as the substrate (Applied Biosystems). The light emission from the cleaved NA-Star substrate was measured for 1s in Envision plate reader (Perkin-Elmer, Wellesley, MA). Neuraminidase activity was determined at 1.7 μM of NA-Star substrate. Enzyme activities were measured as luminescence increases during a 15 min incubation at room temperature.

Determination of IC_{50} of NA Inhibitor. NA inhibition was determined by mixing inhibitor and neuraminidase for 10 min at room temperature followed by the addition of 200 μM of substrate. Inhibitor IC_{50} value were determined from the dose−response curves by plotting the percent inhibition of NA activity versus inhibitor concentrations using Graph Pad Prism 4.

Determination of EC_{50} of NA Inhibitor. The antiflu activities of neuraminidase inhibitors were measured by the EC_{50} values that were the concentrations of NA inhibitor for 50% protection of the H1N1 CPE activities. First, 50 μL of diluted H1N1 at 100 $TCID_{50}$ were mixed with equal volumes of NA inhibitors at varied concentrations. Then the mixtures were used to infect 100 μL of MDCK cells at 1×10^5 cells/mL in 96 wells. After 48 h incubation at 37 °C under 5.0% CO_2, the cytopathic effects (CPE) were determined with CellTiter 96 AQueous Non-Radioactive Cell Proliferation Assay reagent as described above. Inhibitor EC_{50} value were determined by fitting the curve of percent CPE versus the concentrations of NA inhibitor using Graph Pad Prism 4.

Plaque Assay. The virus used in the plaque assay was cultured once from allantoic virus samples. Confluent MDCK cells (70−80%) in 6-well plates were infected with WSN/33 in 0.6 mL of media per well [DMEM with 0.3% bovine serum albumin (Sigma, A9418), 25 mM HEPES, and antibiotics]. The culture plates were placed in 35 °C, 5% CO_2 incubator for virus adsorption for 1 h, washed with medium to remove unbound viruses, and overlaid with 3 mL of 0.4% warm agarose (Uni-Region Bio-Tech, UR-AGA001) in media. The infected cultures were incubated at 35 °C with 5% CO_2 for additional 3 days, fixed with 3.7% formalin, and stained with 0.1% crystal violet solution for plaque visualization.

Acknowledgment. We thank the National Science Council for financial support.

Supporting Information Available: HPLC, ^1H and ^{13}C NMR spectra of new compounds. This material is available free of charge via the Internet at http://pubs.acs.org.

References

(1) Kim, C. U.; Lew, W.; Williams, M. A.; Liu, H.; Zhang, L.; Swaminathan, S.; Bischofberger, N.; Chen, M. S.; Mendel, D. B.; Tai, C. Y.; Laver, W. G.; Stevens, R. C. Influenza neuraminidase inhibitors possessing a novel hydrophobic interaction in the enzyme active site: design, synthesis, and structural analysis of carbocyclic sialic acid analogues with potent anti-influenza activity. *J. Am. Chem. Soc.* **1997**, *119*, 681–690.
(2) Kim, C. U.; Lew, W.; Williams, M. A.; Wu, H.; Zhang, L.; Chen, X.; Escarpe, P. A.; Mendel, D. B.; Laver, W. G.; Stevens, R. C. Structure−activity relationship studies of novel carbocyclic influenza neuraminidase inhibitors. *J. Med. Chem.* **1998**, *41*, 2451–2460.
(3) Lew, W.; Chen, X.; Kim, C. U. Discovery and development of GS 4104 (oseltamivir): an orally active influenza neuraminidase inhibitor. *Curr. Med. Chem.* **2000**, *7*, 663–672.
(4) McClellan, K.; Perry, C. M. Oseltamivir: a review of its use in influenza. *Drugs* **2001**, *61*, 263–283.
(5) von Itzstein, M.; Wu, W.-Y.; Kok, G. B.; Pegg, M. S.; Dyason, J. C.; Jin, B.; Phan, T. V.; Smythe, M. L.; White, H. F.; Oliver, S. W.; Colman, P. M.; Varghese, J. N.; Ryan, D. M.; Woods, J. M.; Bethell, R. C.; Hotham, V. J.; Cameron, J. M.; Penn, C. R. Rational design of potent sialidase-based inhibitors of influenza virus replication. *Nature* **1993**, *363*, 418–423.
(6) Taylor, N. R.; von Itzstein, M. Molecular modeling studies on ligand binding to salidase from influenza virus and the mechanism of catalysis. *J. Med. Chem.* **1994**, *37*, 616–624.
(7) von Itzstein, M.; Dyason, J. C.; Oliver, S. W.; White, H. F.; Wu, W.-Y.; Kok, G. B.; Pegg, M. S. A study of the active site of influenza virus sialidase: an approach to the rational design of novel anti-influenza drugs. *J. Med. Chem.* **1996**, *39*, 388–391.
(8) Dunn, C. J.; Goa, K. L. Zanamivir: a review of its use in influenza. *Drugs* **1999**, *58*, 761–784.
(9) Moscona, A. Neuraminidase inhibitors for influenza. *N. Engl. J. Med.* **2005**, *353*, 1363–1373.
(10) De Clercq, E. Antiviral agents actives against influenza A viruses. *Nat. Rev. Drug Discovery* **2006**, *5*, 1015–1025.
(11) Schmidt, A. C. Antiviral therapy for influenza. *Drugs* **2004**, *64*, 2031–2046.
(12) McKimm-Breschkin, J. L. Resistance of influenza viruses to neuraminidase inhibitors—a review. *Antiviral Res.* **2000**, *47*, 1–17.
(13) Gubareva, L. V.; Webster, R. G.; Hayden, F. G. Comparison of the activities of zanamivir, oseltamivir, and RWJ-270201 against clinical isolates of influenza virus and neuraminidase inhibitor-resistant variants. *Antimicrob. Agents Chemother.* **2001**, *48*, 3403–3408.
(14) de Jong, M. D.; Tran, T. T.; Truong, H. K.; Vo, M. H.; Smith, G. J.; Nguyen, V. C.; Bach, V. C.; Phan, T. Q.; Do, Q. H.; Guan, Y.; Peiris, J. S.; Tran, T. H.; Farrar, J. Oseltamivir resistance during treatment of influenza A (H5N1) infection. *N. Engl. J. Med.* **2005**, *353*, 2667–2672.
(15) Anne Moscona, M. D. Oseltamivir resistance—disabling our influenza defenses. *N. Engl. J. Med.* **2005**, *353*, 2633–2636.
(16) Le, Q. M; Kiso, M.; Someya, K.; Sakai, Y. T.; Nguyen, T. H.; Nguyen, K. H.; Pham, N. D.; Ngyen, H. H.; Yamada, S.; Muramoto, Y.; Horimoto, T.; Takada, A.; Goto, H.; Suzuki, T.; Suzuki, Y.; Kawaoka, Y. Isolation of drug-resistant H5N1 virus. *Nature* **2005**, *437*, 1108.
(17) Shie, J.-J.; Fang, J.-M.; Wang, S.-Y.; Tsai, K.-C.; Cheng, E. Y.-S.; Yang, A.-S.; Hsiao, S.-C.; Su, C.-Y.; Wong, C.-H. Synthesis of

tamiflu and its phosphonate congeners possessing potent anti-influenza activity. *J. Am. Chem. Soc*. **2007**, *129*, 11892–11893.
(18) Shie, J.-J.; Fang, J.-M.; Wong, C.-H. A concise and flexible synthesis of the potent anti-influenza agents tamiflu and tamiphosphor. *Angew. Chem., Int. Ed*. **2008**, *47*, 5788–5791.
(19) Collins, P. J.; Haire, L. F.; Lin, Y. P.; Liu, J.; Russell, R. J.; Walker, P. A.; Skehel, J. J.; Martin, S. R.; Hay, A. J.; Gamblin, S. J. Crystal structures of oseltamivir-resistant influenza virus neuraminidase mutants. *Nature* **2008**, *453*, 1108–1261.
(20) Dharan, N. J.; Gubareva, L. V.; Meyer, J. J.; Okomo-Adhiambo, M.; McClinton, R. C.; Marshall, S. A.; George, K.; Epperson, S.; Brammer, L.; Klimov, A. I.; Bresee, J. S.; Fry, A. M. Infections with oseltamivir-resistant influenza A (H1N1) virus in the United States. *JAMA, J. Am. Med. Assoc*. **2009**, *301*, 1034–1041.
(21) Weinstock, D. M.; Zuccotti, G. The evolution of influenza resistance and treatment. *JAMA, J. Am. Med. Soc*. **2009**, *301*, 1066–1069.
(22) Andrews, D. M.; Cherry, P. C.; Humber, D. C.; Jones, P. S.; Keeling, S. P.; Martin, P. F.; Shawa, C. D.; Swanson, S. Synthesis and influenza virus sialidase inhibitory activity of analogues of 4-guanidino-Neu5Ac2en (zanamivir) modified in the glycerol side-chain. *Eur. J. Med. Chem*. **1999**, *34*, 563–574.
(23) Honda, T.; Masuda, T.; Yoshida, S.; Arai, M.; Kaneko, S.; Yamashita, M. Synthesis and anti-influenza virus activity of 7-*O*-alkylated derivatives related zanamivir. *Bioorg. Med. Chem. Lett*. **2002**, *12*, 1925–1928.
(24) Varghese, J. N.; Laver, W. G.; Colman, P. M. Structure of the influenza virus glycoprotein antigen neuraminidase at 2.9 Å resolution. *Nature* **1983**, *303*, 35–40.
(25) Colman, P. M.; Varghese, J. N.; Laver, W. G. Structure of the catalytic and antigenic sites in the influenza virus neuraminidase. *Nature* **1983**, *303*, 41–44.
(26) Macdonald, S. J. F.; Watson, K. G.; Cameron, R.; Chalmers, D. K.; Demaine, D. A.; Fenton, R. J.; Gower, D.; Hamblin, J. N.; Hamilton, S.; Hart, G. J.; Inglis, G. G. A.; Jin, B.; Jones, H. T.; McConnell, D. B.; Mason, A. M.; Nguyen, V.; Owens, I. J.; Parry, N.; Reece, P. A.; Shanahan, S. E.; Smith, D.; Wu, W.-Y.; Tucker, S. P. Potent and long-acting dimeric inhibitors of influenza virus neuraminidase are effective at a once-weekly dosing regimen. *Antimicrob. Agents Chemother*. **2004**, *48*, 4542–4549.
(27) Watson, K. G.; Cameron, R.; Fenton, R. J.; Gower, D.; Hamilton, S.; Jin, B.; Krippner, G. Y.; Luttick, A.; McConnell, D.; Macdonald, S. J. F.; Mason, A. M.; Nguyen, V.; Tucker, S. P.; Wu, W.-Y. Highly potent and long-acting trimeric and tetrameric inhibitors of influenza virus neuraminidase. *Bioorg. Med. Chem. Lett*. **2004**, *14*, 1589–1592.
(28) Macdonald, S. J.; Cameron, R.; Demaine, D. A.; Fenton, R. J.; Foster, G.; Gower, D.; Hamblin, J. N.; Hamilton, S.; Hart, G. J.; Hill, A. P.; Inglis, G. G. A.; Jin, B.; Jones, H. T.; McConnell, D. B.; McKimm-Breschkin, J.; Mills, G.; Nguyen, V.; Owens, I. J.; Parry, N.; Shanahan, S. E.; Smith, D.; Watson, K. G.; Wu, W. Y.; Tucker, S. P. Dimeric zanamivir conjugates with various linking groups are potent, long-lasting inhibitors of influenza neuraminidase including H5N1 avian influenza. *J. Med. Chem*. **2005**, *48*, 2964–2971.
(29) Yamashita, M.; Tomozawa, T.; Kakuta, M.; Tokumitsu, A.; Nasu, H.; Kubo, S. CS-8958, a prodrug of the new neuraminidase inhibitor R-125489, shows long-acting anti-influenza virus activity. *Antimicrob. Agents Chemother*. **2009**, *53*, 186–192.
(30) Masuda, T.; Yoshida, S.; Arai, M.; Kanedo, S.; Yamashita, M.; Honda, T. Synthesis and anti-influenza evaluation of polyvalent salidase inhibitors bearing 4-guanidino-Neu5Ac2en derivatives. *Chem. Pharm. Bull*. **2003**, *51*, 1386–1398.
(31) Bonnett, R. Photosensitizers of the porphyrin and phthalocyanine series for photodynamic therapy. *Chem. Soc. Rev*. **1995**, *24*, 19–33.
(32) Macdonal, I. J.; Dougherty, T. J. Basic principles of photodynamic therapy. *J. Porphyrins Phthalocyanines* **2001**, *5*, 105–129.
(33) Castano, A. P.; Demidova, T. N.; Hambline, M. R. Mechanism in photodynamic therapy: part one—photosensitizers, photochemistry and cellular localization. *Photodiagn. Photodynam. Ther*. **2004**, *1*, 279–293.
(34) Hamblin, M. R.; Hasan, T. Photodynamic therapy: a new antimicrobial approach to infectious disease?. *Photochem. Photobiol. Sci*. **2004**, *3*, 436–450.
(35) O'Riordan, K.; Akilov, O. E.; Hasan, T. The potential for photodynamic therapy in the treatment of localized infections. *Photodiagn. Photodynam. Ther*. **2005**, *2*, 247–262.
(36) Berthiaume, F.; Reiken, S.; Toner, M.; Tompkins, R.; Yarmush, M. Antibody-targeted photolysis of bacteria in vivo. *Biotechnology* **1994**, *12*, 703–706.
(37) Wainwright, M. Photoinactivation of Viruses. *Photochem. Photobiol. Sci*. **2004**, *3*, 406–411.
(38) Abramson, A. L.; Shikowitz, M. J.; Mullooly, V. M.; Steinberg, B. M.; Amella, C. A.; Rothstein, H. R. Clinical effects of photodynamic therapy on recurrent laryngeal papillomas. *Arch. Otolaryngol. Head Neck Surg*. **1992**, *118*, 25–29.
(39) Shikowitz, M. J.; Abramson, A. L.; Freeman, K.; Steinberg, B. M.; Nouri, M. Efficacy of DHE photodynamic therapy for respiratory papillomatosis: immediate and long-term results. *Laryngoscope* **1998**, *108*, 962–967.
(40) Shikowitz, M. J.; Abramson, A. L.; Steinberg, B. M.; DeVoti, J.; Bonagura, V. R.; Mullooly, V.; Nouri, M.; Ronn, A. M.; Inglis, A.; McClay, J.; Kathrine Freeman, K. Clinical trial of photodynamic therapy with *meso*-tetra (hydroxyphenul) chlorin for respiratory papillomatosis. *Arch. Otolaryngol. Head Neck Surg*. **2005**, *131*, 99–105.
(41) Chandler, M.; Bamford, M. J.; Conroy, R.; Lamont, B.; Patel, B.; Patel, V. K.; Steeples, I. P.; Storer, R.; Weir, N. G.; Wright, M.; Williamson, C. J. Synthesis of the potent influenza neuraminidase inhibitor 4-guanidino Neu5Ac2en. X-Ray molecular structure of 5-acetamido-4-amino-2,6-anhydro-3,4,5-trideoxy-D-erythro-L-gluco-nononic acid. *J. Chem. Soc., Perkin Trans*. **1995**, *1*, 1173–1180.
(42) Ying, L.; Gervay-Hague, J. One-bead-one-inhibitor-one-substrate screening of neuraminidase activity. *ChemBioChem* **2005**, *6*, 1857–1865.
(43) Rostovtsev, V. V.; Green, L. G.; Fokin, V. V.; Sharpless, K. B. A stepwise Huisgen cycloaddition process: copper(I)-catalyzed regioselective "ligation" of azides and terminal alkynes. *Angew. Chem., Int. Ed*. **2002**, *41*, 2596–2599.
(44) Lee, B.-Y.; Parka, S. R.; Jeon, H. B.; Kim, K. S. A new solvent system for efficient synthesis of 1,2,3-triazoles. *Tetrahedron Lett*. **2006**, *47*, 5105–5109.
(45) Lee, Y. C.; Lee, R. T. Carbohydrate−protein interactions: basis of glycobiology. *Acc. Chem. Res*. **1995**, *28*, 321–327.
(46) Mammen, M.; Choi, S. K.; Whitesides, G. M. Polyvalent interactions in biological systems: implications for design and use of multivalent ligands and inhibitors. *Angew. Chem., Int. Ed*. **1998**, *37*, 2755–2794.
(47) Lundquist, J. J.; Toone, E. J. The cluster glycoside effect. *Chem. Rev*. **2002**, *102*, 555–578.
(48) Ohuchi, M.; Asaoka, N.; Sakoi, T.; Ohuchi, R. Roles of neuraminidase in the initial stage of influenza virus infection. *Microb. Infect*. **2006**, *8*, 1287–1293.
(49) Hoffman, A. S Origins and evolution of "controlled" drug delivery systems. *J. Controlled Release* **2008**, *132*, 153–163.
(50) Deckert, P. M. Current constructs and targets in clinical development for antibody-based cancer therapy. *Curr. Drug Targets* **2009**, *10*, 158–175.
(51) Sirion, U.; Kim, H. J.; Lee, J. H.; Seo, J. W.; Lee, B. S.; Lee, S. J.; Oh, S. J.; Chi, D. Y. An efficient F-18 labeling method for PET study: Huisgen 1,3-dipolar cycloaddition of bioactive substances and F-18-labeled compounds. *Tetrahedron Lett*. **2007**, *48*, 3953–3957.
(52) Bonger, K. M.; van den Berg, R. J. B. H. N.; Heitman, L. H.; Ijzerman, A. P.; Oosterom, J.; Timmers, C. M.; Overkleeft, H. S.; van der Marel, G. A. Synthesis and evaluation of homo-bivalent GnRHR ligands. *Bioorg. Med. Chem*. **2007**, *15*, 4841–4856.
(53) Reed, L. J.; Muench, H. A simple method of estimating fifty percent endpoints. *Am. J. Hyg*. **1938**, *27*, 493–497.
(54) Burleson, F. G.; Chambers, T. M.; Wiedbrauk, D. L. Virology, a Laboratory Manual; Academic Press: San Diego, CA, 1992.